

# 直流無刷馬達及其驅動控制

(Brushless DC Motor and Its Driving Control)

廖 聰 明  
清華大學 電機系  
(94.07)

1

## I. Classification of PMSMs

- Surface-mounted PMSM (SPMSM)
- Interior SPMSM (IPMSM)
  - ☒ Permanent magnet rotor with magnetic saliency.
  - ☒ Advantages:
    - High power density.
    - Excellent acceleration ability.
    - Low operating noise.
    - High reliability.
    - Suitable for high speed operation due to rigid rotor structure.
  - ☒ Limitations:
    - Existence of *cogging torque*.
    - Nonlinear inductance characteristic.
    - Higher cost.

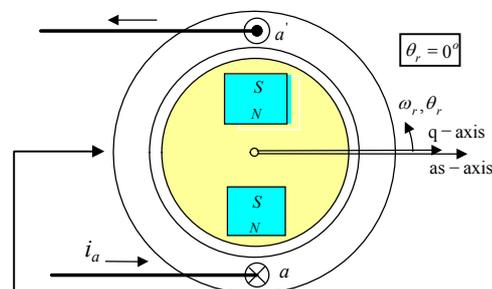
2

### 不同馬達應用於空調機之性能比較：

- 四種馬達：IM, SynRM, SPMSM, IPMSM
- 比較之性能：Cogging torque、轉矩特性、效率及損失、成本。
- (i) 齒隙轉矩(Cogging torque)：IPMSM與SPMSM具有Cogging torque，其中IPMSM較大，因其具有凸極效應(Saliency)，在壓縮機負載之應用上，應具有有效小之Cogging torque，因需具有低噪音及低振動特性；
- (ii) 馬達效率及損失：IPMSM之效率最高，因其除具永磁轉矩外，尚具有磁阻轉矩，其所需之定子電流最小，而具有最小之銅損。SPMSM無磁阻轉矩，其銅損增大。另外，因外包鋼膜上之感生渦流所造成之鐵損，以及較大之氣隙，使其效率稍低。而SynRM因無永磁轉矩，全靠磁阻轉矩而效率較低，但仍比IM高約2~3%；
- (iii) 成本：以SynRM為1.0當比較對象，IM、IPMSM、SPMSM分別為其之1.13、1.42、1.5倍。由上之比較可知，欲得高性能高效率之空調運轉操控特性，可選用IPMSM，而如欲得最低成本者，可選用SynRM，只是效率較低，但仍比IM高些。 3

### ◆ 磁凸極對線圈電感之影響：

由於IPM轉子具有永久磁石及凸極效應，且磁石之導磁係數遠小於鐵心之導磁係數 ( $\mu_m < \mu_c$ )，亦即  $R_m > R_c$ ，使得IPM之q軸電感不等於d軸電感 ( $L_q > L_d$ )。電樞電感值為轉子位置 ( $\theta_r$ ) 之非線性函數，且此電感值亦與激磁頻率和激磁電流之準位有相當之關聯。線圈電感與轉子位置之關係：

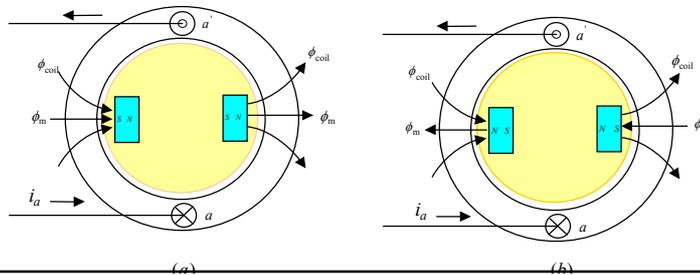


Winding inductance

4

### ◆ 外加激磁下d軸阻抗之變化：

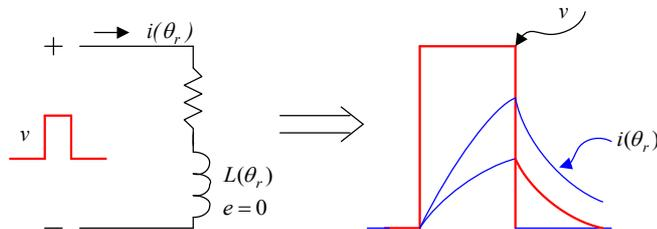
- ☒ 利用磁飽合效應從事轉子磁極位置之偵測。
- ☒ **原理：**當飽合程度增加時， $L_d$  下降，則在一樣之外加電壓下所造成之電流將增加，在圖(a)中，線圈造成之磁通與磁鐵之磁通為相同方向，線圈磁通與磁鐵磁通具相加成之作用，此時  $L_d$  變小(飽合)；而圖(b)中，線圈磁通與磁鐵磁通方向相反，有相互抵消之作用，此時  $L_d$  大。據此，我們可以判別出磁極位置。



5

### ◆ 利用磁飽合效應從事轉子磁極極性之判斷及位置偵測

- ☒ 在線圈兩端外加一短脈寬之脈波電壓信號，由量測之電流從事轉子位置估測及磁極極性之判斷。



- ☒ 在三相線圈注入高頻諧波電壓(電流)，由量測之電流(電壓)信號從事轉子位置估測及磁極極性之判斷。

6

## ◆ 轉矩產生特性及換向調控

- 同步磁阻馬達(SynRM):  $\Phi_f = 0 \Rightarrow$

最大轉矩產生角發生在:  $\beta_{max} = \theta_{r,max} = 45^\circ$

- 表面貼磁式直流無刷馬達(SPM) :

$\Phi_f \neq 0, L_d - L_q = 0 \Rightarrow \beta_{max} = \theta_{r,max} = 0^\circ$

- IPMSM 直流無刷馬達:

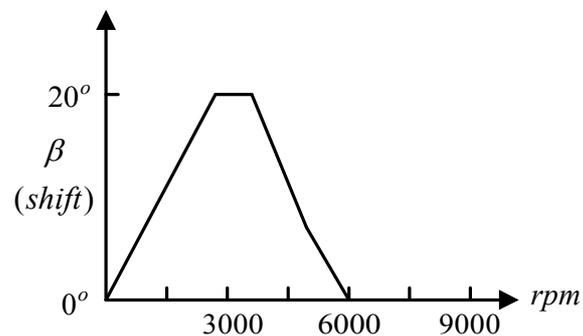
$\Phi_f \neq 0, L_d - L_q \neq 0 \Rightarrow \beta_{max} = \theta_{r,max} = 0^\circ \sim 45^\circ$

$$\beta_{max} = \sin^{-1} \frac{\sqrt{\Phi_f^2 + 32L_1^2 I_a^2} - \Phi_f}{8L_1 I_a}, \quad L_1 = \frac{\Delta L_q - L_d}{2}$$

7

## 最佳 $\beta$ 角對轉速之概略關係

- 實際上,  $\beta_{max}$  與速度、負載、馬達參數等均有關。
- $\beta$  角之調控: 須特別研究的課題為採用合適之方法及合適之性能評估指標(Performance index)來做換向調控以達到較佳之操控性能。



8

## 激磁調控

- 對IPMSM而言，由於  $L_d \neq L_q$ ，所以若要產生最佳轉矩或最大之TPI (Torque per current)，不令  $i_d = 0$

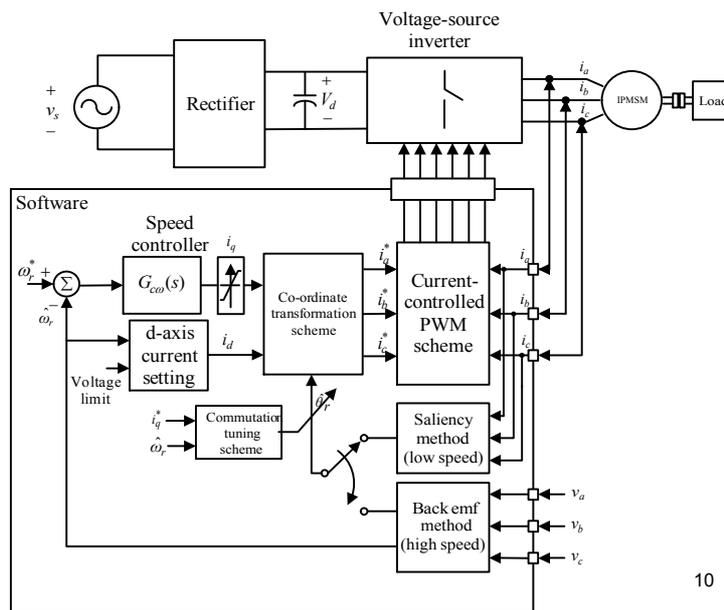
- $\omega_r \leq$  額定速度：
$$i_d = \frac{\Phi_f}{2(L_q - L_d)} - \sqrt{\frac{\Phi_f^2}{4(L_q - L_d)^2} + i_q^2}$$

- $\omega_r >$  額定速度：
$$i_d = -\frac{\Phi_f}{L_d} + \frac{1}{L_d} \sqrt{\frac{(V_m)^2}{(\frac{P}{2})^2 \omega_r^2} - L_q^2 i_q^2}$$

用以行弱磁控制

9

## ◆ Sensorless BDCM using IPMSM



10

## II. STRUCTURE AND GOVERNING EQUATIONS

### ■ Classification of BDCMs

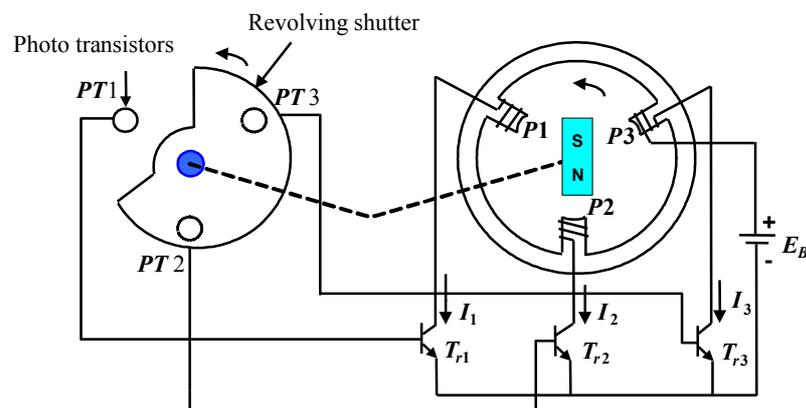
#### ☒ Speed servo drive: square-wave BDCM

- Using photo sensor
- Using Hall sensor

#### ☒ Position servo drive: sine-wave BDCM

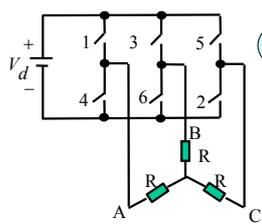
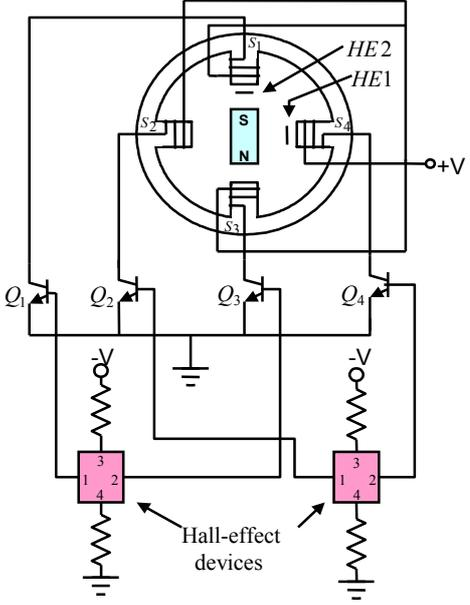
11

### ■ Square-wave BDCM: using photo sensor



12

■ Square-wave BDCM: using Hall sensor

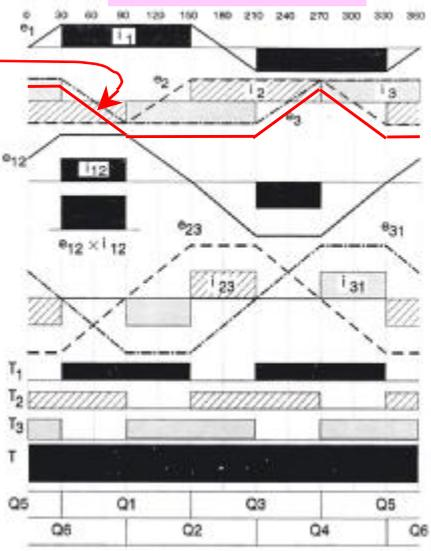


Non-conducting phase back-EMF

$$P_m = \sum e_k i_k = T_e \omega_r$$

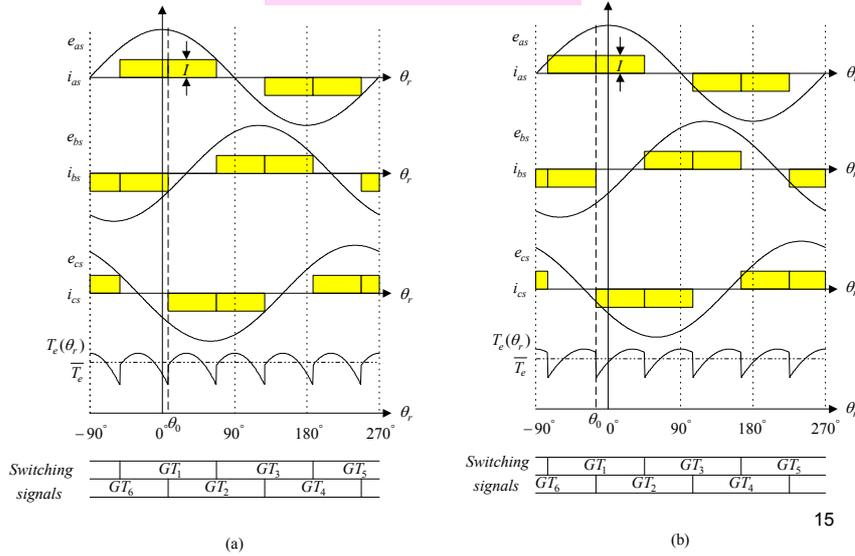
$$T_e = T_L + B \omega_r + J \frac{d\omega_r}{dt}$$

- Ideal waveforms of a Y-connected BDCM with 120° flat-top back EMF.
- Non-ideal winding current and voltage waveforms and commutation ⇒ yielding torque ripple.



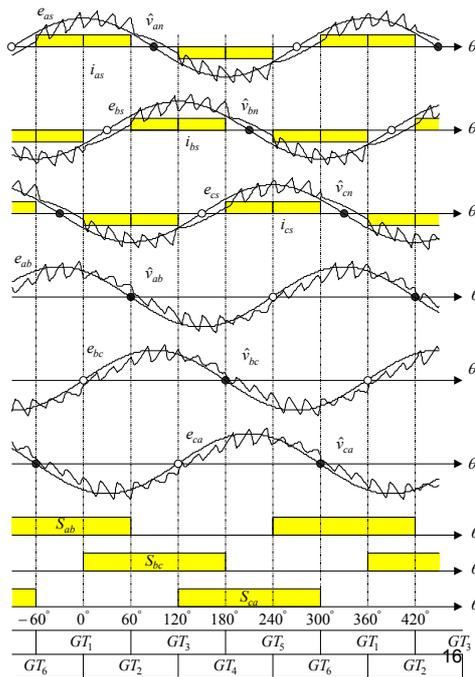
■ Effect of commutation instant on torque generation of BDCM

(a)  $\theta_0 > 0^\circ$ ; (b)  $\theta_0 < 0^\circ$ .

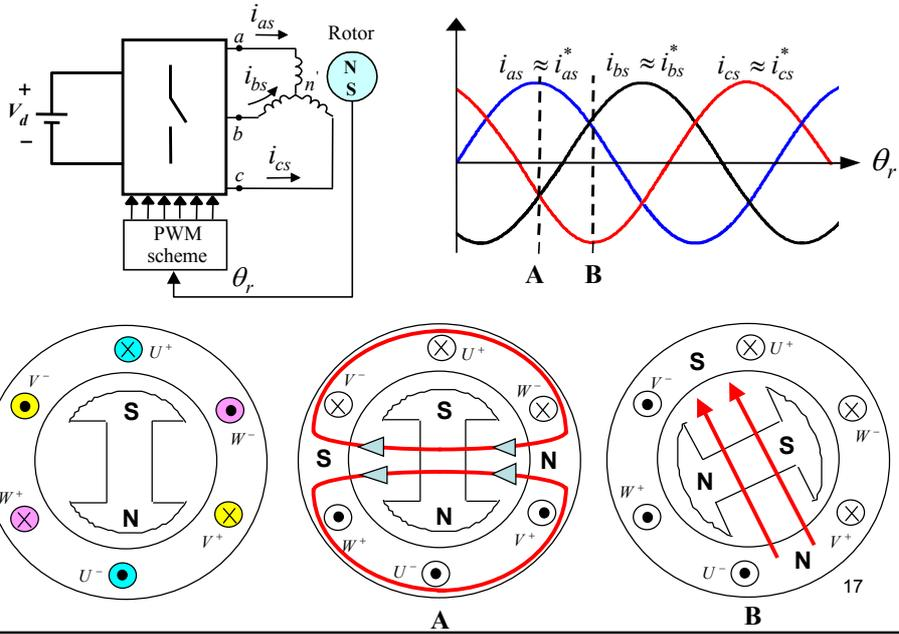


15

The sketched waveforms of hypothetical back-EMFs, filtered terminal voltages and gating signals.

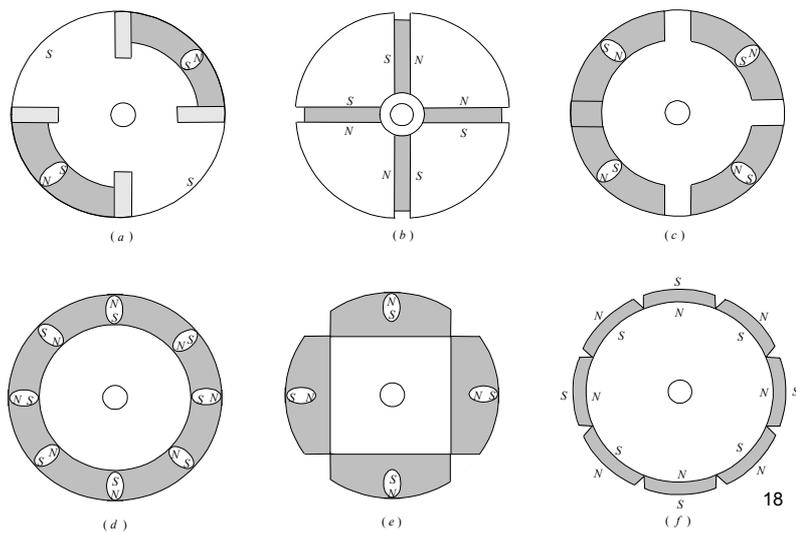


## ■ Operating principle of sine-wave BDCMs



## ■ Structure of PMSMs

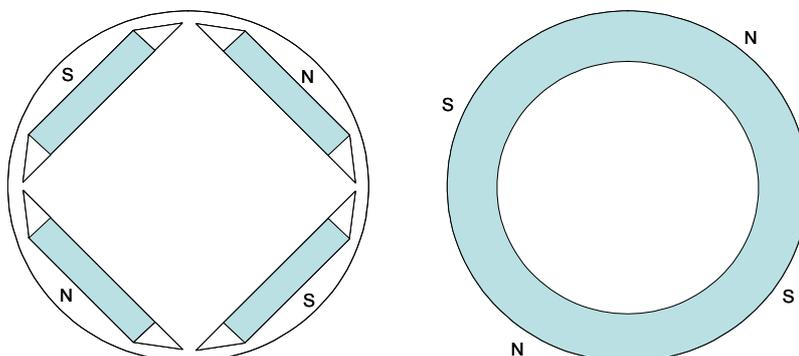
⊗ Rotor



- (1) As shown in Fig. 2.2(a), the N poles are formed on the rotor back iron between magnets. Although the number of magnets is reduced to half, the length of magnets must be increased. Owing to non-uniform material on the rotor surface, both the reluctance torque and cogging torque exist.
- (2) The structure shown in Fig. 2.2(b) is a common rotor model of the IPMSM. The magnetic flux enters into the air gap through soft-iron. If the cross sectional area of magnet is larger than the surface area of the soft-iron around the air gap, the flux concentration will occur. This type of rotor also possesses reluctance and cogging torques. Recently, there have been many types of rotor structures with multi-layer magnets being developed.
- (3) As shown in Fig. 2.2(c), the nonmagnetic spacer between the magnets is replaced by electrical steel, this will lead to the increase of reluctance torque component.
- (4) Fig. 2.2(d) shows a rotor structure without spacers. The rotor is constructed from a single piece of bonded magnetic material, which is magnetized with alternating magnet poles. The major advantage of this type of rotor is low cost.
- (5) Figs. 2.2(e) and 2.2(f) show two rotor structures of SPMSM. The efficiencies of these types of rotors are lower due to their larger air gap and the induced eddy current due to the steel-sleeve mounted on the rotor surface.

19

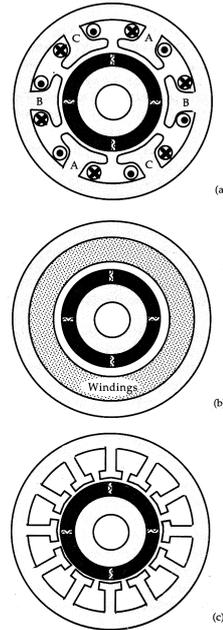
- 內置式磁石同步馬達其他常見之轉子型式。
- 環型磁鐵轉子型式。



20

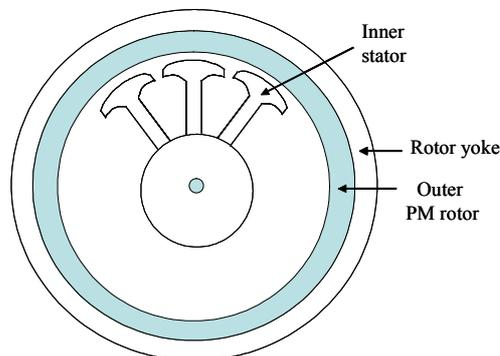
## ☒ Stator

- (a) 如圖(a)，為salient pole：具有短的end turns，相與相間之coupling較小，每一相之線圈不同時，與所有轉子磁鐵作用時，導致性能之降低。
- (b) 如圖(b)，沒有slot (Slot-less)，故沒有齒隙轉矩(Cogging torque)，但線圈與後鐵間之熱導低，不利負荷之增加。又因沒有靜子齒，使得氣隙增長成轉子表面至後鐵，為維持適當大之PC值，磁鐵之長度須增長。
- (c) 如圖(c)，具有shoes在氣隙處，可減少氣隙磁導隨位置之變化，而減少cogging torque。



### 外永磁轉子(Outer rotor)、內電樞定子馬達：

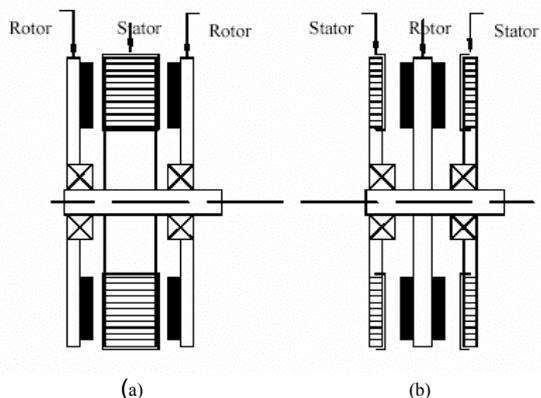
外永磁轉子(Outer rotor)、內電樞定子，電樞繞組採集中(Concentrated)式，具繞組繞製較簡易、銅損較小、可薄型化、散熱較不易、轉矩漣波較大等特點。由於具有較大之氣隙處半徑力臂，有較大之轉矩產生能力，但需有降低轉矩漣波及噪音之對策考量。常用於散熱扇、電動車輛、電梯、升降梯、磁碟機主軸驅動等，需馬達為扁平薄型化之場合。



22

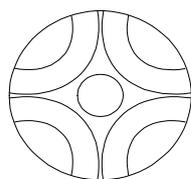
## ■ 軸向磁通(Axial flux)馬達

軸向磁通馬達為扁平薄型化馬達，常用於電腦週邊裝置之驅動，又稱(Pan-cake motor)，定子電樞及永磁轉子可為單側式及雙側式，電樞繞組有時為印刷式，稱為 (Printed circuit board motors)。

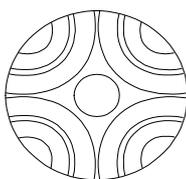


23

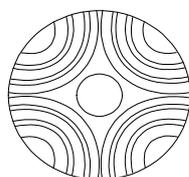
## Multi-layer rotor structure of IPMSM



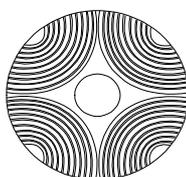
(a) Single-layer



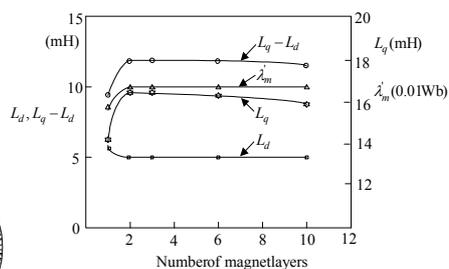
(b) Two-layer



(c) Four-layer



(d) Ten-layer



☒ Two-layer IPMSM possesses better compromised performance

24

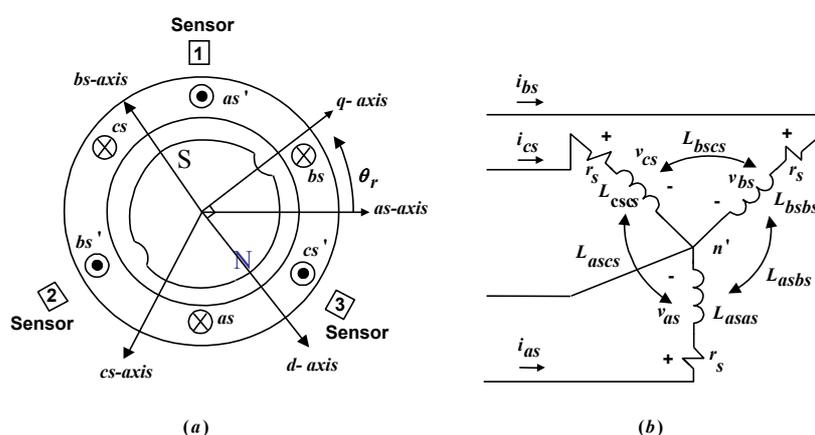
## 永久磁鐵及磁路分析

永久磁鐵已有多種材質，各有其去磁特性，一些典型永磁材質之特性比較於圖3。在永磁磁路之安排與磁路分析上，須注意磁路之組態與材質，以及氣隙之形狀與尺寸。如圖4所示，永磁磁路之磁通密度永久磁鐵之去磁特性與磁路之Shear line決定之。又溫度亦極影響其操作點偏磁之大小。由線圈之磁動勢安匝產生之磁力線流通於永磁磁極間，使其產生電磁轉矩，磁力線之流通路徑，由於間隙之存在而有邊緣效應(Fringing effect)、鐵心之飽和及非線性激磁特性，使得準確之磁路分析較為困難達成。一般常須仰賴有限元(Finite element)模擬分析，然而其複雜、模式須妥當建立且執行演算較慢。故亦常應用簡易之磁阻等效電路法。如能考慮週延，可得較為精確之簡化等效電路，亦可用於磁路分析與設計之進行。

25

## Governing equations

☒ The configuration and conventional definition of IPMSM



26

☒ **The armature voltage equation**

$$v_{abc s} = r_s i_{abc s} + \frac{d\lambda_{abc s}}{dt}$$

☒ **The flux linkages equations**

$$\lambda_{as} = L_{asas} i_{as} + L_{asbs} i_{bs} + L_{ascs} i_{cs} + \lambda'_m \sin \theta_r$$

$$\lambda_{bs} = L_{bsas} i_{as} + L_{bsbs} i_{bs} + L_{bscs} i_{cs} + \lambda'_m \sin(\theta_r - \frac{2\pi}{3})$$

$$\lambda_{cs} = L_{csas} i_{as} + L_{csbs} i_{bs} + L_{cscs} i_{cs} + \lambda'_m \sin(\theta_r + \frac{2\pi}{3})$$

27

☒ **Voltage equations in rotor reference frame**

$$v_{qd0s}^r = r_s i_{qd0s}^r + \omega_r \lambda_{dqs}^r + p \lambda_{qd0s}^r$$

☒ **Expanded forms**

$$v_{qs}^r = r_s i_{qs}^r + \omega_r \lambda_{ds}^r + p \lambda_{qs}^r$$

$$v_{ds}^r = r_s i_{ds}^r - \omega_r \lambda_{qs}^r + p \lambda_{ds}^r$$

$$v_{0s}^r = r_s i_{0s}^r + p \lambda_{0s}^r$$

where

$$\lambda_{qs}^r = L_q i_{qs}^r, \quad \lambda_{ds}^r = L_d i_{ds}^r + \lambda'_m$$

$$L_q = L_{ls} + \frac{3}{2}(L_A + L_B), \quad L_d = L_{ls} + \frac{3}{2}(L_A - L_B)$$

28

⊗ The developed torque

$$T_e = \frac{3P}{2} \left[ \lambda_m^r I_{as} \cos \beta - (L_d - L_q) I_{as}^2 \sin \beta \cos \beta \right]$$

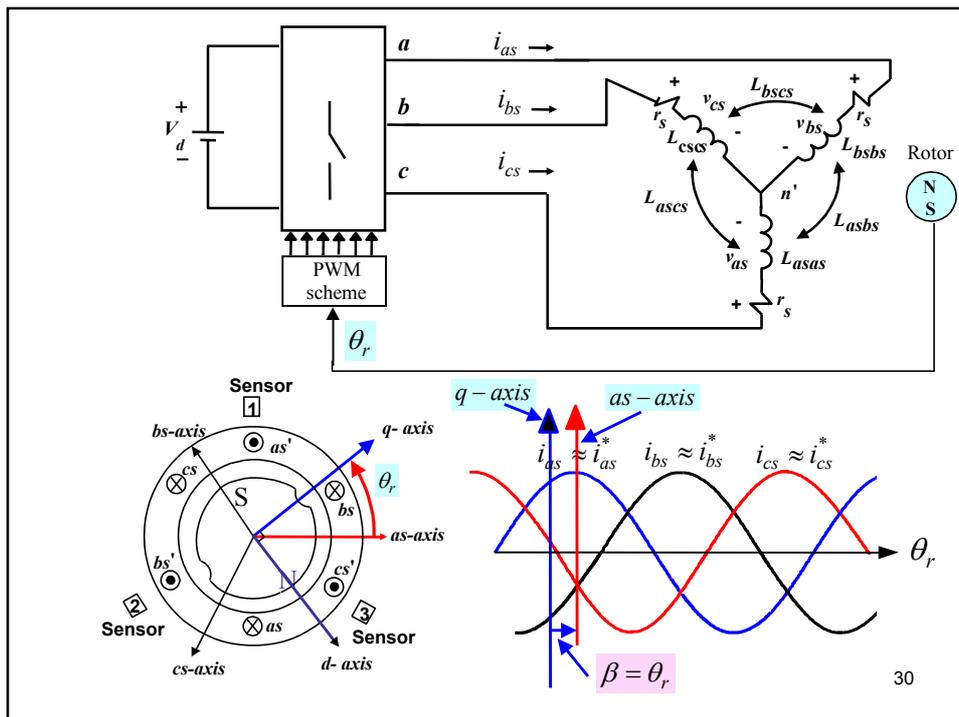
$$= \frac{3P}{2} \left[ \lambda_m^r I_{as} \cos \beta + \frac{L_q - L_d}{2} I_{as}^2 \sin 2\beta \right]$$

Electromagnetic torque

Reluctance torque

■ For an IPMSM, its developed torque consists of both electromagnetic torque and reluctance torque due to  $L_d \neq L_q$

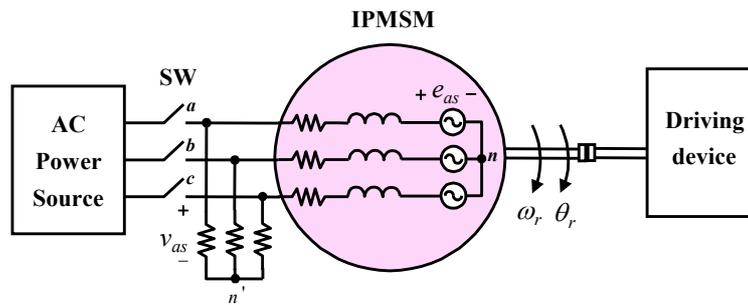
29



30

### III. ESTIMATION OF EQUIVALENT CIRCUIT PARAMETERS

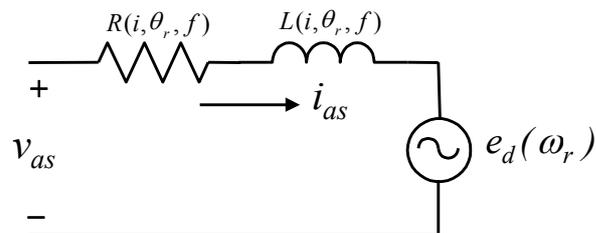
■ **Experimental mechanism for making parameter estimation**



- Rotor is locked at a particular position and the winding is excited with a variable-frequency and variable-current AC source.
- The voltage, current and power are recorded.

31

■ **Per-phase equivalent circuit model**



- ☒ **Back EMF constant estimation:**

$$e_d = k_t \omega_r$$

- ☒ **Flux linkage amplitude estimation:**  $\lambda'_m$

32

## ☒ Winding inductances

$$L_{asas} = L_{ls} + L_A + L_B \cos 2\theta_r$$

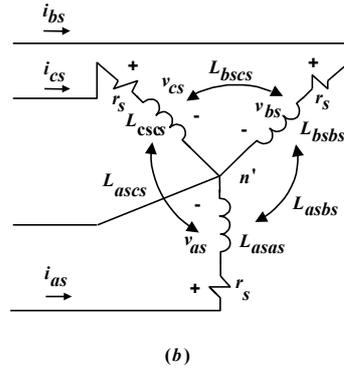
$$L_{bsbs} = L_{ls} + L_A + L_B \cos 2\left(\theta_r - \frac{2\pi}{3}\right)$$

$$L_{csbs} = L_{ls} + L_A + L_B \cos 2\left(\theta_r + \frac{2\pi}{3}\right)$$

$$L_{asbs} = L_{bsas} = -\frac{1}{2}L_A + L_B \cos 2\left(\theta_r - \frac{\pi}{3}\right)$$

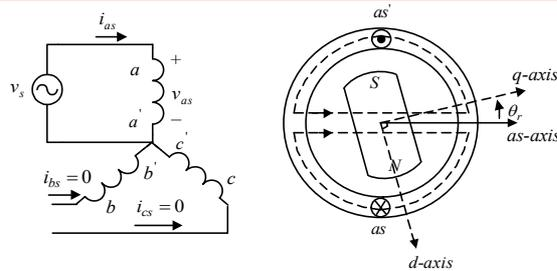
$$L_{ascs} = L_{csas} = -\frac{1}{2}L_A + L_B \cos 2\left(\theta_r + \frac{\pi}{3}\right)$$

$$L_{bscs} = L_{csbs} = -\frac{1}{2}L_A + L_B \cos 2(\theta_r + \pi)$$



33

## ■ Y-connected with non-isolated neutral



$$\boxed{\otimes} \quad v_s = v_{as} = r_s i_{as} + \frac{d}{dt} [(L_{ls} + L_A + L_B \cos 2\theta_r) i_{as}] = r_s i_{as} + \frac{d}{dt} [L_{asas}(\theta_r) i_{as}]$$

$$L_{asas, \max} = L_{asas}(\theta_r = 0) = L_{ls} + L_A + L_B$$

$$L_{asas, \min} = L_{asas}(\theta_r = 0.5\pi) = L_{ls} + L_A - L_B$$

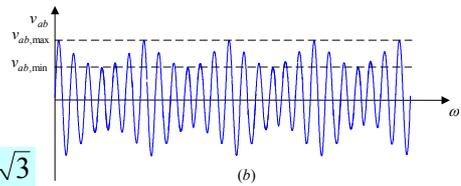
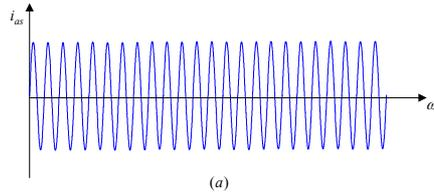
$$L_q \approx \frac{3}{2} L_{asas, \max}, \quad L_d \approx \frac{3}{2} L_{asas, \min}$$

$$L_q \overset{\Delta}{=} L_{ls} + \frac{3}{2}(L_A + L_B), \quad L_d \overset{\Delta}{=} L_{ls} + \frac{3}{2}(L_A - L_B)$$

34

## Parameter estimation via slip test

- ☒ Stator is excited by a three-phase current source, and rotor is driven at a speed slightly different from the synchronous speed.
- ☒ Synchronous rotating flux encounters different reluctance paths.



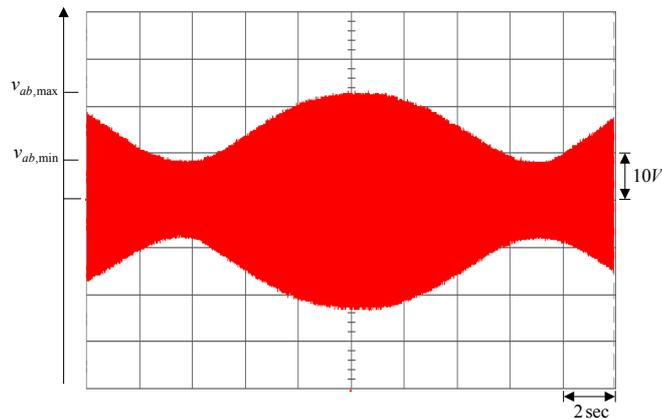
$$Z_d = \frac{v_{ab,\min} / \sqrt{3}}{\sqrt{2}I_L}, \quad Z_q = \frac{v_{ab,\max} / \sqrt{3}}{\sqrt{2}I_L}$$

$$L_d = \frac{\sqrt{Z_d^2 - r_s^2}}{\omega}, \quad L_q = \frac{\sqrt{Z_q^2 - r_s^2}}{\omega}$$

35

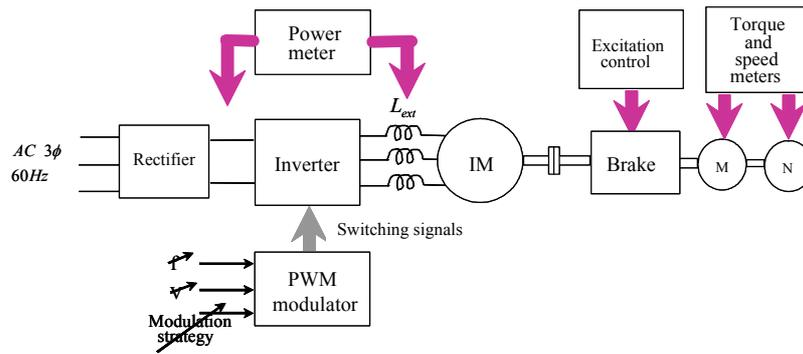
## 滑差測試

- 滑差測試所量得之線電壓波形



36

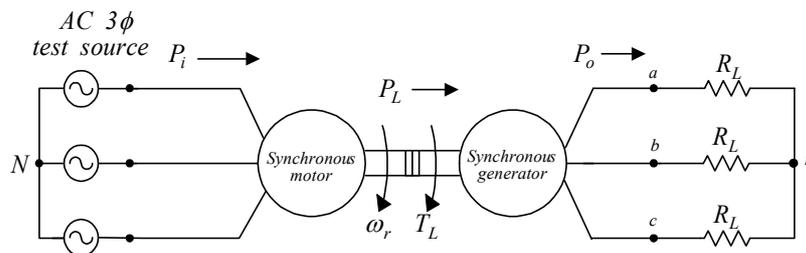
## 馬達之運轉性能估測



37

## 替代方案：(應用兩相同馬達對耦接)

$$\eta = \sqrt{P_o/P_i}, \quad P_L = P_o/\eta, \quad T_L = P_L/\omega_r$$

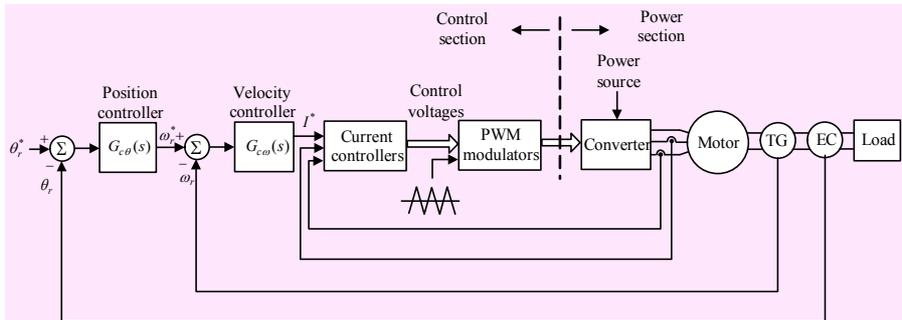


38

## IV. 以DSP為主之IPMSM直流無刷馬達驅動系統

### ■ Typical motor drive system configuration:

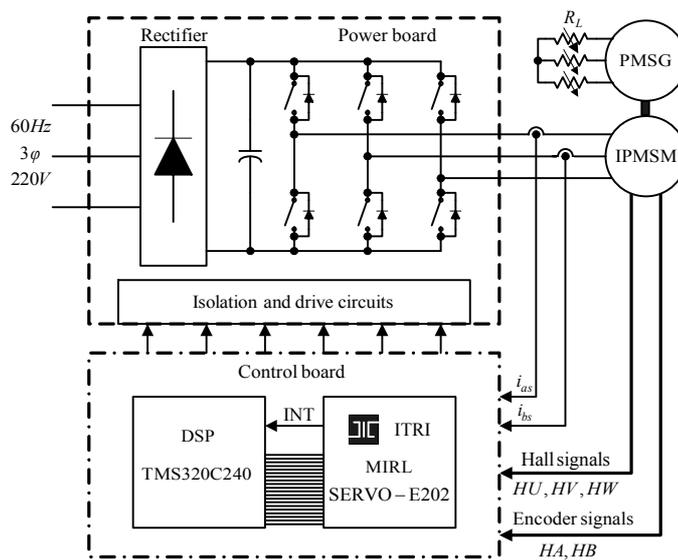
**Multi-loop: position loop, velocity loop, current, loop  
PWM switching scheme**



### ■ Some practical digital control issues

39

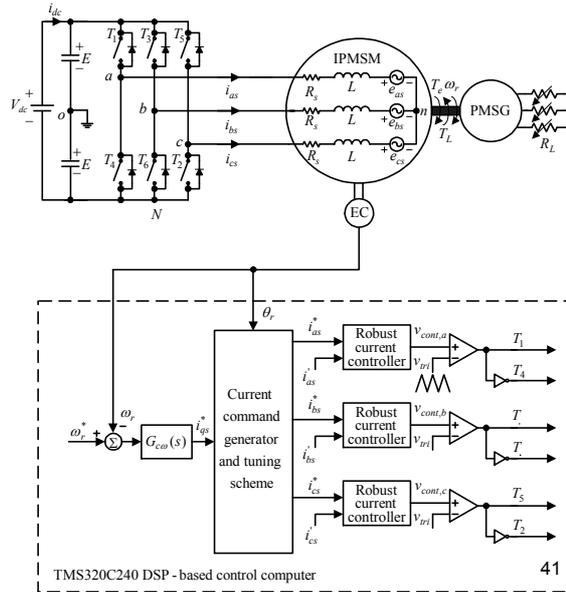
## DSP-based motor drive



40

## V. ROBUST CURRENT CONTROL, EXCITATION AND COMMUTATION TUNING

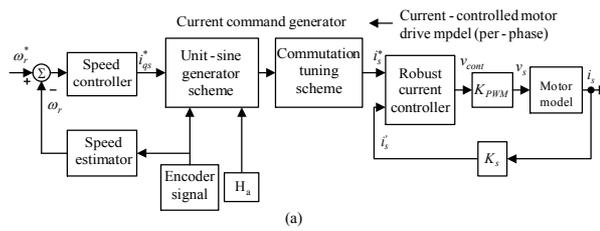
System configuration  
IPMSM drive



TMS320C240 DSP - based control computer

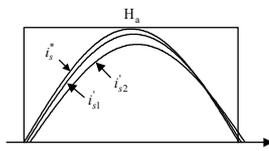
41

## ■ 所提之控制理念



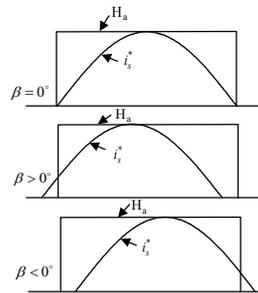
(a)

⊗ 線圈電流  
控制波形：



(b)

⊗ 換相時刻  
調整：



(c)

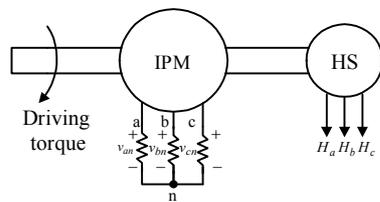
42

## 換相時刻調整

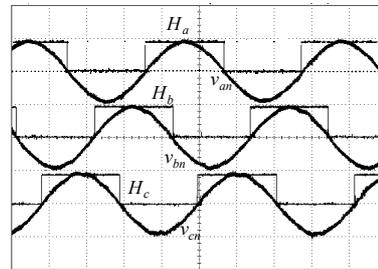
### ■ 相位校準及霍爾感測信號

- 機械對位調整
- 電氣對位調整

霍爾位置感測信號相位調校之機構



調整後量測所得之感測馬達之開路端電壓



43

## 激磁及換相時刻調整對轉矩產生能力之影響

### ■ 激磁調整及換相時刻調整間之等值性

對一固定之電樞電流 ( $I_a = \text{constant}$ )，產生最大轉矩之角度可由令  $\partial T_e / \partial \beta = 0$  求之，為：

$$\beta = \beta_{\max} = \sin^{-1} \frac{-\lambda'_m + \sqrt{\lambda_m'^2 + 8(L_q - L_d)^2 I_{as}^2}}{4(L_q - L_d) I_{as}}$$

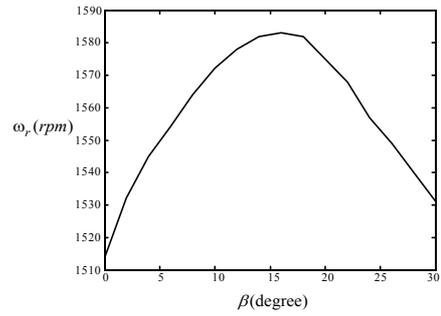
在下  $\beta_{\max}$ ，對應之d-axis 電流為  $i_{ds}^r = -I_{as} \sin \beta_{\max}$

$$i_{ds}^r = \frac{\lambda'_m}{2(L_q - L_d)} - \sqrt{\frac{\lambda_m'^2}{4(L_q - L_d)^2} + i_{qs}^r{}^2}$$

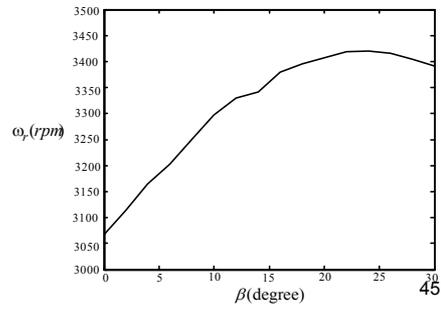
44

## 換相時刻之離線 (off-line)調整

- 在不同之  $\beta$  值下量測之速度 ( $R_L = 20\Omega$ ) :
  - (a)  $i_{qs}^* = 7A$  ( $I_{as,rms} = 5A$ ) ;
  - (b)  $i_{qs}^* = 3.5A$  ( $I_{as,rms} = 2.5A$ ) 。

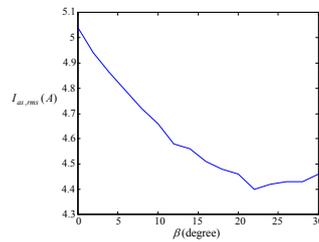
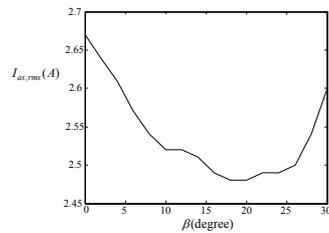


(a)

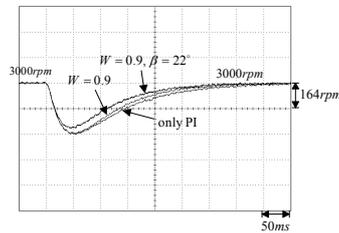
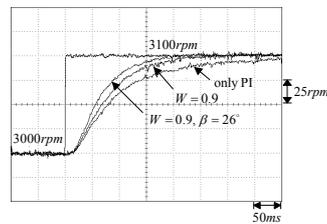


(b)

(a) 在不同之  $\beta$  值下量測之馬達線電流，(3000rpm,  $R_L = 40\Omega$ ) (上)及 (3000rpm,  $R_L = 20\Omega$ ) (下)；(b) 速度步級命令變化(3000rpm  $\rightarrow$  3100rpm,  $R_L = 20\Omega$ ) (上)及步級負載電阻變化( $R_L = 40\Omega \rightarrow R_L = 20\Omega$ , 3000rpm) (下)量測所得之速度響應比較。



(a)

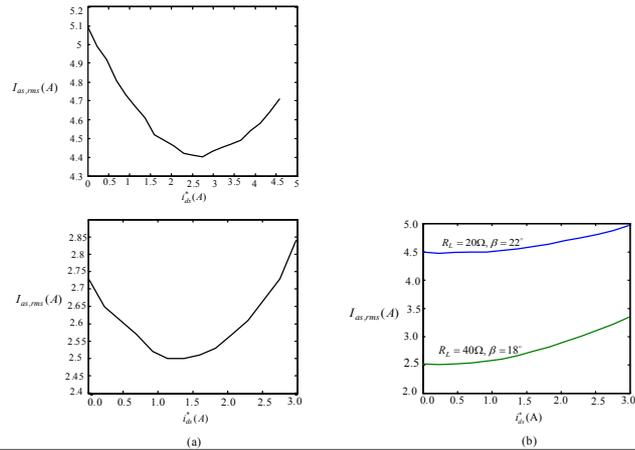


(b)

46

## 激磁電流之離線(off-line)調整

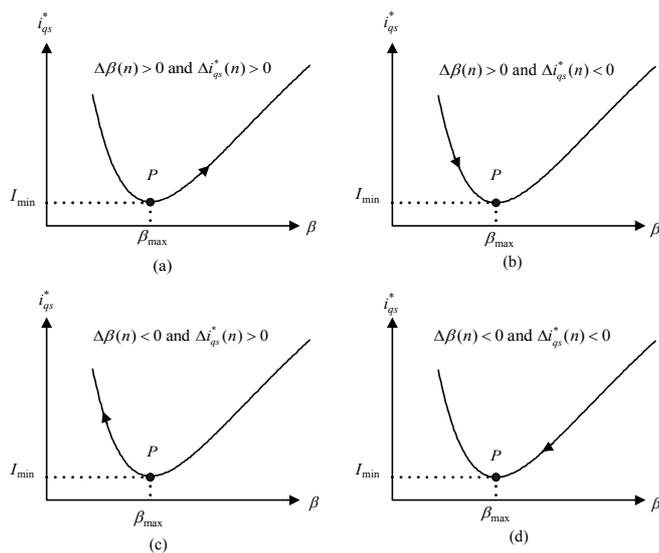
(a) 設定在(3000rpm,  $R_L = 40\Omega$ )(上)及(3000rpm,  $R_L = 20\Omega$ )(下)穩態定速運轉下，在不同之值下量測之馬達線電流；(b) 設定在  $\beta_{\max}$  附近 ( $\beta = 18^\circ$ , 3000rpm,  $R_L = 40\Omega$ ) and ( $\beta = 22^\circ$ , 3000rpm,  $R_L = 20\Omega$ )，在不同  $i_{ds}^*$  之值下量測之馬達線電流。



47

## 換相時刻之智慧調控

### ■ 變化換相時刻角度所造成 $i_{qs}^*$ 之變化



48

## 換相時刻角度調控法則

$$\beta(n+1) = \beta(n) - k_p \text{sign}(\Delta\beta(n)) \Delta i_{qs}^*(n)$$

$$\text{sign}(\Delta\beta(n)) = \begin{cases} 1 & \text{for } \Delta\beta(n) \geq 0 \\ -1 & \text{for } \Delta\beta(n) < 0 \end{cases}$$

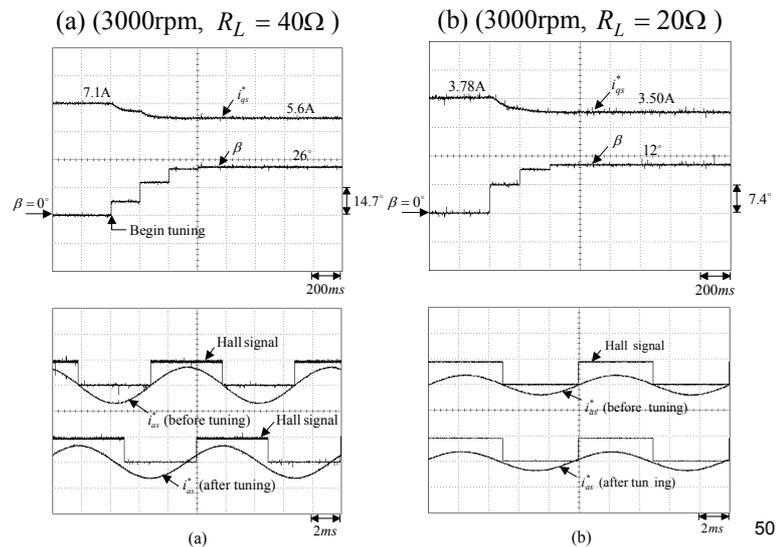
$k_p$  = 靈敏度(Sensitivity)之調整用增益

$$\Delta i_{qs}^*(n) = i_{qs}^*(n) - i_{qs}^*(n-1)$$

$$\Delta\beta(n) = \beta(n) - \beta(n-1)$$

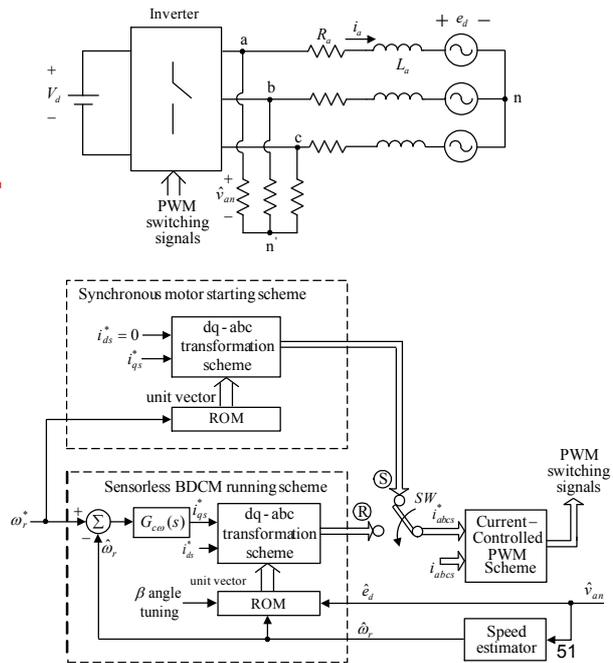
49

● 在  $\beta$  值調控前及調控後，量測之  $i_{qs}^*$ ,  $\beta$ ,  $H_a$



50

# Sensorless IPMSM drive



## Starting process

Bump-less starting is needed

